Journal of Quantitative Spectroscopy & Radiative Transfer 110 (2009) 1879–1893

Contents lists available at ScienceDirect

Journal of Quantitative Spectroscopy & Radiative Transfer

journal homepage: www.elsevier.com/locate/jqsrt

Radiation characteristics of *Botryococcus braunii*, *Chlorococcum littorale*, and *Chlorella sp.* used for CO_2 fixation and biofuel production

Halil Berberoglu [a], Pedro S. Gomez [b], Laurent Pilon [b,*]

[a] University of Texas, Austin, Cockrell School of Engineering, Mechanical Engineering Department, Austin, TX 78712-0292, USA
[b] University of California, Los Angeles, Henri Samueli School of Engineering and Applied Science, Mechanical and Aerospace Engineering Department, Los Angeles, CA 90095-1597, USA

ARTICLE INFO

Article history:
Received 20 November 2008
Received in revised form
8 April 2009
Accepted 11 April 2009

Keywords:
Radiative transfer
Scattering
Photobioreactors
Carbon dioxide fixation
CO_2 mitigation
Flue gas
Bioscrubber
Controlled ecological life support systems

ABSTRACT

This paper reports experimental measurements of the radiation characteristics of green algae used for carbon dioxide fixation via photosynthesis. The generated biomass can be used to produce not only biofuels but also feed for animal and food supplements for human consumptions. Particular attention was paid to three widely used species namely *Botryococcus braunii*, *Chlorella sp.*, and *Chlorococcum littorale*. Their extinction and absorption coefficients were obtained from normal–normal and normal–hemispherical transmittance measurements over the spectral range from 400 to 800 nm. Moreover, a polar nephelometer was used to measure the scattering phase function of the microorganisms at 632.8 nm. It was observed that for all strains, scattering dominates over absorption. The magnitudes of the extinction and scattering cross-section are functions of the size, shape, and chlorophyll content of each strain in a non-trivial manner. Absorption peaks at 435, 475, and 676 nm corresponding to chlorophyll *a* and chlorophyll *b*. The results can be used for scaling and optimization of CO_2 fixation in ponds or photobioreactors as well as in the development of controlled ecological life support systems.

1. Introduction

Intensive use of fossil fuels increases concentration of carbon dioxide in the atmosphere and contributes to world climate changes [1]. For example, 71.4% of the electricity consumed in the US is generated from fossil fuels [2]. Electricity generation alone contributed to 33% of the total CO_2 emissions of the country in 2006 which itself represents about 23% of the total world emission [3]. Flue gasses from fossil fuel power plants consist of 4–14 vol% of CO_2 and up to 200 ppm of NO_x and SO_x depending on the type of fuel and on the combustion process [4]. Overall, the concentration of CO_2 in the atmosphere in 2006 varied between 360 and 390 parts per million by volume (ppmv) during the year and feature a continuous increase year after year [5]. It is predicted that CO_2 levels above 450 ppm in the atmosphere will have severe impact on sea levels, global climate patterns, and survival of many species and organisms [1].

Current technologies for mitigating CO_2 can be divided in three groups namely (1) storage, (2) utilization, and (3) fixation. The most common method of capturing CO_2 is monoethanolamine scrubbing [4]. Other storage technologies

* Corresponding author. Tel.: +1 310 206 5598; fax: +1 310 206 4830.
E-mail address: pilon@seas.ucla.edu (L. Pilon).

0022-4073/$ - see front matter © 2009 Elsevier Ltd. All rights reserved.
doi:10.1016/j.jqsrt.2009.04.005

Nomenclature

$A_{abs,\lambda}$	spectral absorption cross-section (m^2)
$E_{ext,\lambda}$	spectral extinction cross-section (m^2)
g	Henyey–Greenstein asymmetry factor
I_λ	radiance (intensity) ($W/m^2\,\mu m\,sr$)
L	cuvette path length (m)
n	refractive index
N	microorganism cell density ($\#/m^3$)
OD	optical density
$\hat{s}$	local spatial coordinate unit vector
$S_{sca,\lambda}$	spectral scattering cross-section of microorganisms (m^2)
t	sample thickness (m)
T	transmittance (%)
X	microorganism concentration (kg/m^3)
x	size parameter

Greek letters

β	extinction coefficient (1/m)
Θ	scattering angle (rad)
κ	absorption coefficient (1/m)
λ	wavelength (nm)
Ω	solid angle (sr)
σ	scattering coefficient (1/m)
τ	non-dimensional optical thickness
Φ	scattering phase function

Subscripts

λ	refers to wavelength
h	refers to normal–hemispherical measurements
HG	refers to Henyey–Greenstein phase function
PBS	refers to phosphate buffer saline solution

include (a) underground geological cavity at a depth of 6–800 m [6] as well as (b) surface [4] or (c) deep ocean injection [7], (d) desiccant adsorption [8], and (e) molecular sieve technology [9]. Unfortunately, these storage methods suffer from major challenges including (i) the separation and compression of CO_2, (ii) the development of efficient pumping methods, (iii) uncertainties in the long term stability of the stored CO_2, (iv) possible severe negative impact on the environment [4], and/or (v) the capital and energy costs [10].

Utilization technologies either use CO_2 as is from industrial processes or convert it into useful products via chemical processes. For example, difficult to extract oil and natural gas can be forced out of the ground through injection of CO_2 into the fields [4]. Liquid CO_2 has solvent properties and can be used in various industrial processes as an alternative to organic solvents. CO_2 can be reduced to both liquid such as methanol [11] and gaseous fuels such as methane [12] via thermochemical or electrochemical processes.

Fixation is a biochemical process where CO_2 is stored in a stable organic form through photosynthesis. Terrestrial vegetation and soil as well as the oceans are natural sinks for CO_2 [4]. The methods for increasing the rate of CO_2 sequestration through enhancement of natural sinks are (i) afforestation [13], (ii) ocean fertilization, (iii) rock weathering enhancement, (iv) algae culture in photobioreactors, and (v) artificial photosynthesis. The CO_2 consumption rate of trees vary by tree type and location. Although there are no adverse effects of this option to the ecosystem, locating and dedicating arable land for afforestation can conflict with population growth, freshwater supply, and food production for human consumption [14,4]. In oceans, microorganisms such as phytoplankton fix CO_2 into biomass at a rate of 50–100 Gt-C per year [4]. This is a much higher rate than that of terrestrial vegetation which ranges from 5 to 10 Gt-C per year [4]. However, this process is limited by the availability of nutrients such as nitrogen, phosphate, silicate, and iron to the microorganisms [15,16]. Thus, fertilizing the oceans locally with these limiting nutrients can result in enhanced phytoplankton production and CO_2 uptake [15,16]. Although promising results were obtained in field experiments [4], this option has excessive interference with the ecosystem and can have fatal impact on other marine life [17]. In addition, the sinking and decaying biomass can release stronger greenhouse gases to the atmosphere such as methane and nitrogen dioxide [17]. Rock weathering enhancement involves carbonation of silicate rocks containing calcium or magnesium [4]. The final product is calcium or magnesium carbonate which are in solid form [18]. However, this fixation process is very slow making the natural rock weathering process impractical for industrial CO_2 sequestration [19]. Artificial photosynthesis consists of reproducing natural photosynthetic processes in a more straightforward and efficient way [20]. This approach is still in its infancy and efficiency and reliability remain major challenges.

Microalgae cultivation in photobioreactors addresses many of the above mentioned challenges. They have larger photosynthetic efficiencies than higher plants (e.g., trees or sugar cane) [21]. Kurano et al. [22] has demonstrated that microalgae *Chlorococcum littorale* can fix up to 0.85 kg CO_2/m^3/day in a 20 l tubular photobioreactor having a footprint area of 6.6×10^{-2} which is equivalent to 25.6 kg C/m^2/year compared with 0.3–0.9 kg C/m^2/year for trees [14,23]. Microalgae require 140–200 kg of water per kilogram of C fixed compared with more than 550 kg of water per kg of CO_2 fixed by trees [14]. Unlike for trees, water for microalgae can be low quality (waste water) and even high salinity water both unsuitable for agriculture use or human consumption [14]. Thus, cultivation of these microorganisms in photobioreactors offers a sustainable method for carbon dioxide capture and storage [24–27] suitable in semi-arid or arid lands without competing with human habitat or agriculture production [14]. In addition, CO_2 fixation using microalgae grown in photobioreactors does not require CO_2 capture, separation (concentration), and, scrubbing of SO_x and NO_x prior to using the flue gas from fossil fuel power plants. Finally, microalgae produce value-added by-products which can make the processes more economical. For example, some algal species are already used in medicinal and pharmaceutical products as well as health

drinks for their immuno-stimulatory, antioxidant, antiviral, and anticancer activities [28]. Others are incorporated in novel materials or used as fertilizer, in animal feed, in aquaculture, and stock material for biofuels [29,27].

Challenges in photosynthetic CO_2 mitigation include the relatively low efficiency and scaling of the system from bench top to industrial scale. Biological barriers such as growth inhibition due to excessive CO_2 concentration and tolerance to high temperature, NO_x and SO_x or toxic environment can be addressed by screening wild strains or through genetic engineering [30,31]. Similarly, light availability to optimally perform photosynthesis is essential to achieving the maximum efficiency possible [32,33]. In order to design, optimize, and scale up photobioreactors to maximize CO_2 fixation and sunlight energy conversion efficiency and thus minimize water usage, one needs to determine the optical properties (or radiation characteristics) of the microalgae of interest. This paper presents the optical properties of some of the most promising algae for CO_2 fixation and production of biofuels and other added-value products. The reported properties will be useful for the scaling and optimization of the CO_2 fixation in ponds or photobioreactors as well as in the development of controlled ecological life support systems (CELSS) for space exploration missions [34,35].

2. Current state of knowledge

2.1. CO_2 consuming microorganisms

Photosynthesis is a multi-step process by which plants and algae fix carbon dioxide into sugar using sunlight. Particularly, the step of photosynthesis at which CO_2 is converted to sugar with the help of ATP (adenosine-5′-triphosphate) is known as Calvin cycle. The overall reaction for photosynthesis is given by

$$CO_2 + H_2O + light \rightarrow (CH_2O)_n + O_2 \tag{1}$$

Green algae are eukaryotic organisms that can perform photosynthesis. Just like plants, they use water as their electron source, sunlight as their energy source, and CO_2 as their carbon source. In turn they produce oxygen and carbohydrates, protein, and lipids contained within the cells. They are typically more efficient than higher plant at converting solar energy into biomass thanks to their simple cellular structure and the readily available supply of CO_2 and various nutrients dissolved in water. Thus, microalgae can produce 30 times more oil than terrestrial oilseed crops for a given surface area [36].

This study focuses on three microorganisms of particular interest for CO_2 mitigation and biofuel productions namely (i) *Botryococcus braunii* (ii) *Chlorella sp.*, (iii) *C. littorale* [37,25]. *B. braunii* is a pyramid shaped planktonic microalga. Although it is a unicellular species, *B. braunii* forms colonies that are held together by lipid biofilms [38]. It is interesting for its high lipid content in the form of hydrocarbon (up to 43% by dry cell weight) which can be converted into biofuels [39,40,36,41]. It grows in freshwater and can be used as feedstock for hydrocracking in oil refinery to produce gasoline, kerosene, and diesel [42]. Moreover, *Chlorella sp.* is a unicellular green algae, ellipsoidal in shape with an average major and minor diameter of 12 and 9.5 μm, respectively. It has a high oil content (up to 32% by dry cell weight) and is widely considered for CO_2 sequestration due to its fast growth rate under large CO_2 concentrations [41,43,44]. The marine green algae *C. littorale* is a spherical unicellular strain with cells of diameter about 10 μm. It is of interest for its tolerance to high CO_2 concentrations and the fact that it can grow to very large cell density [45,46]. Hu et al. [46] have demonstrated a CO_2 consumption rate of 16.7 g of CO_2 per liter of a flat-plate photobioreactor per day at a light intensity of 2000 $\mu mol/m^2/s$ at 25 °C and cell density of 80 kg/m^3.

The US Department of Energy Aquatic Species Program performed from 1978 to 1996 concluded the following [36]: (1) "significant potential land, water, and CO_2 resources exist to support this technology", (2) culture of biofuel producing algae is likely to be performed in open ponds due to the low cost required to make this technology competitive. Recently, air lift photobioreactors have been demonstrated at pilot scale to reduce CO_2 emissions of a 20 MW natural gas fired cogeneration power plant [47] and a 1060 MW combined cycle gas turbine power plant [48].

2.2. Radiation transfer through microorganisms suspensions

Solar radiation transfer within absorbing, scattering, and non-emitting media, such as microorganism suspensions in photobioreactors or open ponds, is governed by the radiative transport equation (RTE). The RTE is a semi-empirical integro-differential equation derived from energy conservation considerations. For a given wavelength λ, it is expressed in terms of dimensionless optical coordinates as [49]

$$\frac{dI_\lambda}{d\tau_\lambda} = -I_\lambda(\tau_\lambda,\hat{s}) + \frac{\omega_\lambda}{4\pi}\int_{4\pi} I_\lambda(\tau_\lambda,\hat{s}_i)\Phi_\lambda(\hat{s}_i,\hat{s})\,d\Omega_i \tag{2}$$

where I_λ is the spectral radiance (often called spectral intensity [49]) expressed in $Wm^{-2}\,\mu m^{-1}sr^{-1}$. Here, $\hat{s}$ is the unit vector in the line-of-sight direction and $d\Omega_i$ is the solid angle around $\hat{s}_i$. The dimensionless optical thickness τ_λ and the single scattering albedo ω_λ are defined, respectively, as

$$\tau_\lambda = \int_0^s (\kappa_\lambda + \sigma_\lambda)\,ds = \int_0^s \beta_\lambda\,ds \quad \text{and} \quad \omega_\lambda = \frac{\sigma_\lambda}{\kappa_\lambda+\sigma_\lambda} = \frac{\sigma_\lambda}{\beta_\lambda} \tag{3}$$

where κ_λ, σ_λ, and β_λ ($=\kappa_\lambda+\sigma_\lambda$) are the absorption, scattering, and extinction coefficients, respectively, and expressed in m^{-1}. The scattering phase function $\Phi_\lambda(\hat{s}_i,\hat{s})$ represents the probability that the radiation propagating in direction $\hat{s}_i$ be scattered in direction $\hat{s}$, and is normalized such that

$$\frac{1}{4\pi}\int_{4\pi}\Phi_\lambda(\hat{s}_i,\hat{s})\,d\Omega_i=1 \tag{4}$$

Note that, in the ocean optics literature, the variables κ_λ, σ_λ, β_λ, and Φ_λ are often denoted by a_λ, b_λ, c_λ, and β_λ, respectively [50–52]. In the present study, the nomenclature commonly used in the radiative heat transfer community is employed [49].

Eq. (2) indicates that the absorption and scattering coefficients, or the extinction coefficient and the single scattering albedo, together with the scattering phase function are major parameters needed to solve the radiation transfer equation and predict light transfer in photobioreactors or ponds for simulation, design and optimization purposes. However, these characteristics are strongly dependent on wavelength and difficult to predict from electromagnetic wave theory given the complex morphology of the microorganisms and their various chromophores.

The extinction and absorption coefficients of microorganisms as well as the scattered intensity can be directly measured experimentally. Agrawal and Mengüç [53] offered a comprehensive review of the experimental techniques for measuring these parameters. The radiation characteristics of aquatic microorganisms have been measured and reported in the literature with particular applications to ocean optics [50,54], solar radiation conversion to algae [55,56] and more recently for photobiological hydrogen production [57,58].

Under single scattering regime, the radiation characteristics of microorganisms are linearly dependent on concentration [59]. Thus, it is more convenient to use the average extinction and absorption cross-sections of a microorganism, denoted by $E_{ext,\lambda}$ and $A_{abs,\lambda}$, respectively, and expressed in m^2. They are defined as [59]

$$E_{ext,\lambda}=\frac{\beta_\lambda}{N}\quad\text{and}\quad A_{abs,\lambda}=\frac{\kappa_\lambda}{N} \tag{5}$$

where N is the concentration of the microorganisms expressed in number of cells per m^3 of liquid medium. Similarly, the scattering coefficient σ_λ and the scattering cross-section $S_{sca,\lambda}$ expressed in m^2 are defined as

$$\sigma_\lambda=\beta_\lambda-\kappa_\lambda\quad\text{and}\quad S_{sca,\lambda}=\frac{\sigma_\lambda}{N}=E_{ext,\lambda}-A_{abs,\lambda} \tag{6}$$

The extinction coefficient β_λ is obtained from normal–normal transmittance measurements of dilute suspensions [49]. A large body of literature exists on measuring the absorption coefficient κ_λ both in the field (in situ) and in the laboratory [60–62]. In situ measurements usually deal with extremely small concentrations of microorganisms and setups are designed to overcome this difficulty by increasing the path length of the sample.

To the best of our knowledge, this study presents, for the first time, experimental measurements of the radiation characteristics of microalgae considered for CO_2 fixation and biofuel production over the spectral range from 400 to 800 nm as well as their scattering phase function at 632.8 nm.

3. Materials and methods

3.1. Microorganism cultivation and sample preparation

The freshwater species *B. braunii* UTEX 572 and *Chlorella sp*. UTEX EE90 were purchased from the culture collection of algae at the University of Texas at Austin, TX, USA (UTEX) and received as living cultures on agar slants. They were cultivated in Modified Bold 3N Medium. The salt water species *C. littorale* MBIC 10280 was purchased from the Japanese Society for Culture Collection (JSCC, Japan) and received as a living culture in liquid medium. *C. littorale* was cultivated in 5% F/2 medium [63]. All strains were grown under an irradiance of 2000–3000 lux provided by fluorescent light bulbs (Ecologic by Sylvania, USA). Samples were taken from actively growing cultures of each strain during their exponential growth phase. In order to eliminate the absorption and scattering by the nutrient media, the microorganisms were centrifuged at 2000 rpm for 5 min, washed, and suspended in phosphate buffer saline (PBS) solution.

Fig. 1 shows micrographs of the three species considered. In addition, the cell size distribution has been quantified for each strain using a 100 μm deep hemacytometer (Hausser Scientific, USA, Model 1490) and the image processing and analysis software Image J [64]. The software approximates the cells as ellipsoids and reports the primary and secondary axes as major and minor diameters. More than 400 cells were counted for each strain. Fig. 2 shows the number frequency of the major and minor diameters of the cells for all strains with bins 0.1 μm in width. Table 1 summarizes the average major and minor diameters and the associated standard deviation for each strain. It also reports the average (i) circularity defined as $C=4\pi A/P$, where A and P are the projected area and perimeter of the cell, respectively, and (ii) the Feret diameter defined as the longest distance between two points along the perimeter of a particle [64].

Microorganism concentrations were determined using calibration curves that relate the optical density (OD) at 750 nm of a microorganism suspension to both the dry cell weight X (in kg/m^3) and the number of cells per unit volume of liquid N

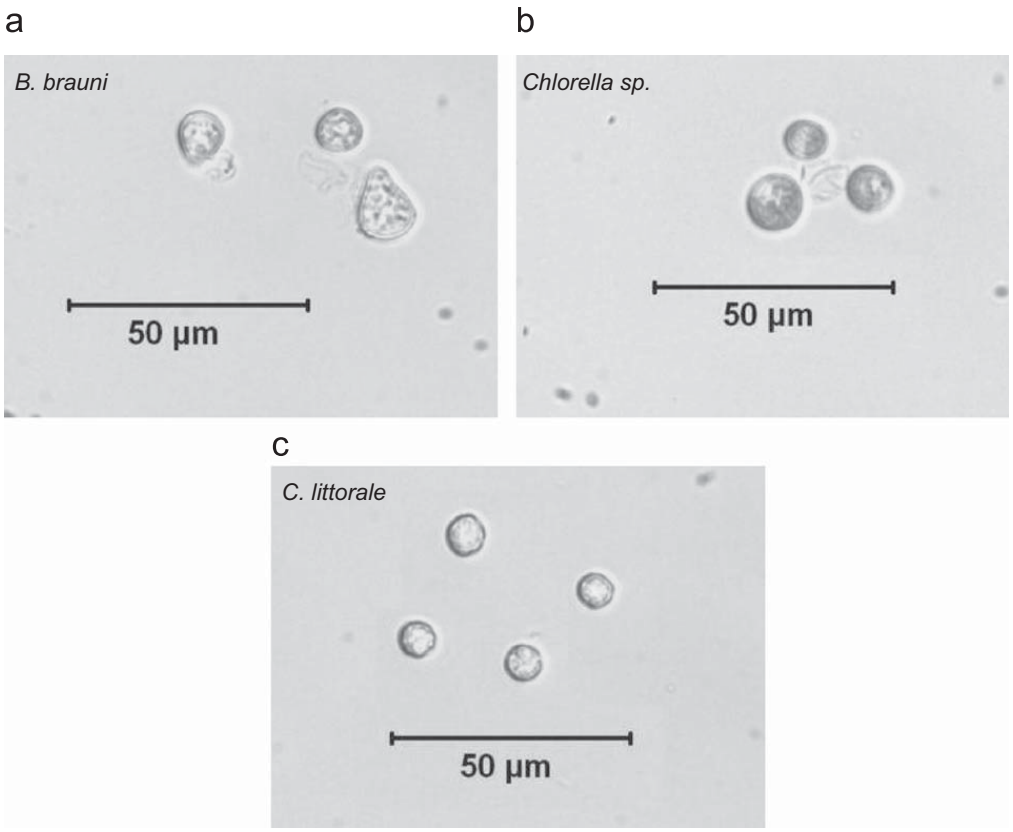

Fig. 1. Micrographs of (a) *B. braunii*, (b) *Chlorella sp.*, and (c) *C. littorale*.

(in cells/m^3). The optical density is defined at 750 nm as $OD = -\log_{10}(T_{750}/T_{750,PBS})$, where T_{750} and $T_{750,PBS}$ are the transmittances at 750 nm of the microorganism suspended in PBS and of PBS alone, respectively. The calibration curves were created by measuring the dry cell weight and the number of cells per unit volume for a given value of OD. First, the OD of the microorganisms was measured at 750 nm in disposable polystyrene cuvettes with path length of 10 mm [27] using a UV–Vis spectrophotometer (Cary-3E by Varian, USA). Then the cells were counted using the hemacytometer and Image J software. Finally, the microorganism suspensions were filtered through mixed cellulose filter membranes with 0.45 μm pore size (HAWP-04700 by Millipore, USA) and dried at 85 °C over night. The dried filters were weighed immediately after being taken out of the oven on a precision balance (model AT261 by Delta Range Factory, USA) with a precision of 0.01 mg. Fig. 3 shows calibration curves for N and X versus OD at 750 nm using a 1 cm path length cuvette. It enables conversion between these commonly used units. The cell number density combined with microorganism shape, size distribution, and chlorophyll content is important for theoretically predicting radiation characteristics of algal suspensions [65].

Finally, the chlorophyll *a* and chlorophyll *b* concentrations were determined for each strain using the ethanol extraction method developed by Wintermans and De Mots [66]. Measurements were performed at least at four different times between two consecutive transfers. The chlorophyll *a* and chlorophyll *b*, and total chlorophyll concentrations, expressed in gram of chlorophyll per kilogram dry cell of microorganism, are reported in Table 1 for the three microorganisms considered. *B. braunii* features significantly larger Chl *a* and Chl *b* concentrations as also suggested by the calibration curves shown in Fig. 3. *C. littorale* has Chl *a* concentration similar to that of *Chlorella sp.* but larger Chl *b* concentration. *C. littorale* algae are also smaller and it remains unclear how their radiation characteristics will compare.

3.2. Experimental procedure and analysis

In measuring the radiation characteristics, the following assumptions were made: (1) the microorganisms were well mixed (i.e., randomly distributed) and randomly oriented, (2) for all measurements, the path length and the concentration of the samples were such that single scattering prevails, i.e., photons underwent one scattering event at most as they travel through the suspension, (3) the scattering phase function had azimuthal symmetry and was only a function of the polar angle [49]. Moreover, the scattering phase function for large particles does not vary significantly with wavelength at scattering angles less than 15° [50]. Most of the scattered light is in the forward direction and phase function

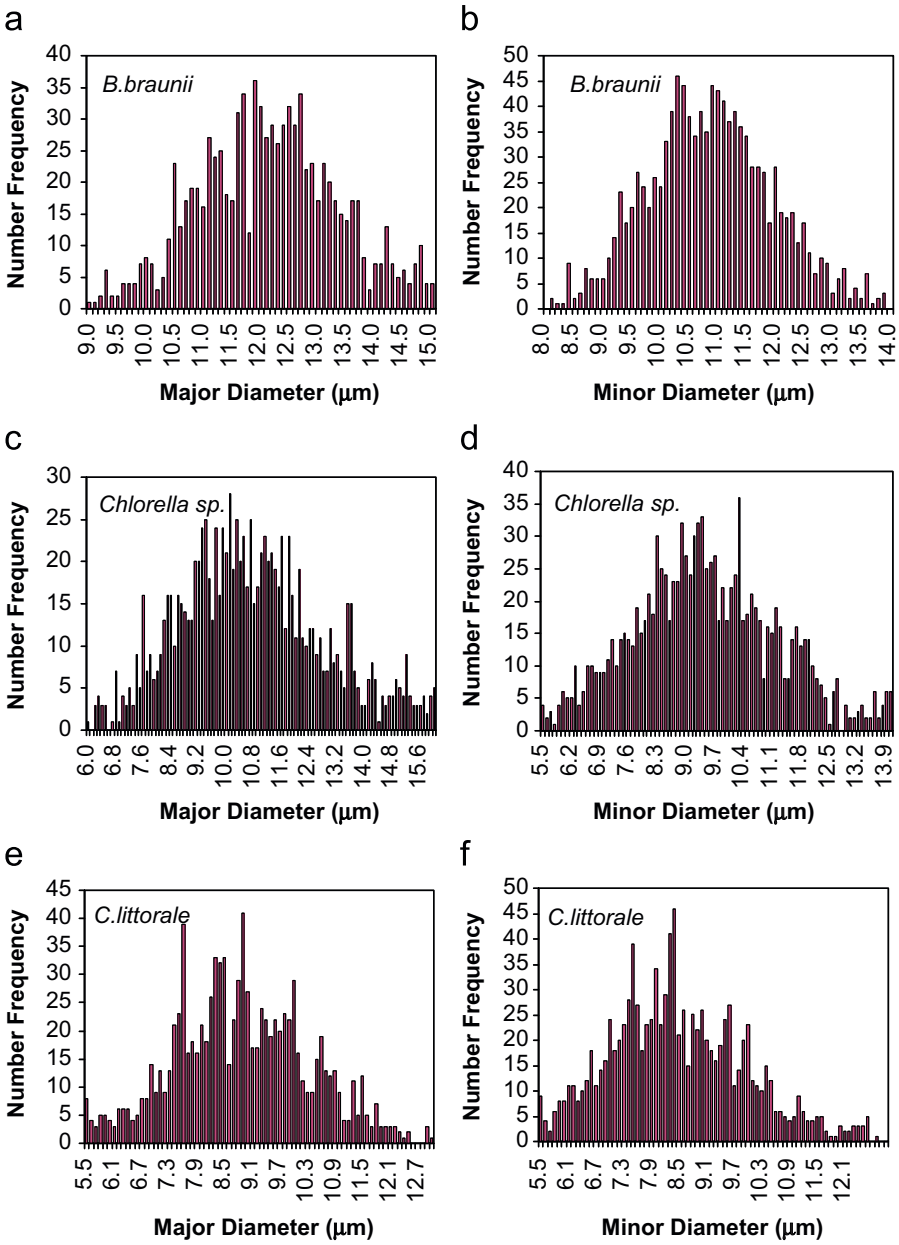

Fig. 2. Measured number frequency of the major and minor cell diameters for (a, b) *B. braunii*, (c, d) *Chlorella sp.*, and (e, f) *C. littorale*.

measurements taken at 632.8 nm can be used as a first order approximation for modeling light transfer in photobioreactors over the photosynthetically active region (PAR) ranging from 400 to 700 nm.

The scattering phase function at 632.8 nm was measured by a polar nephelometer. Details of the experimental setup and the associated analysis have been reported elsewhere [57] and need not be repeated. Validation was performed with Latex microspheres 5 and 19 μm in diameter and randomly oriented fibers 17 μm in diameter and about 1 cm long to treat them as infinitely long. Good agreement was observed between experimental data and results predicted from the Mie theory for spheres [67] and infinitely long and randomly oriented cylinders [68].

The extinction coefficient β_λ of each species was measured from normal–normal transmittance measurements $T_{\lambda,X}$ over the spectral range from 400 to 800 nm using a UV–VIS–NIR spectrophotometer (Shimadzu, USA, Model UV-3101PC). The results were corrected for the portion of the light scattered in the forward direction and detected by the spectrophotometer in directions other than the normal direction due to the finite size of the acceptance angle [58].

Finally, the absorption coefficient κ_λ was determined from the hemispherical transmittance measurements performed with an integrating sphere [55] combined with the same UV–VIS–NIR spectrophotometer used for measuring β_λ. The measurements were corrected for scattering errors using the analysis suggested by Davies-Colley [51]. The experimental

Table 1
Mean diameters, their standard deviations, circularity, and Feret diameter along with the Henyey–Greenstein asymmetry factor of the CO_2 consuming microorganisms investigated.

	B. braunii	*Chlorella sp.*	*C. littorale*
Average major diameter (μm)	13.3	12.0	9.6
Standard deviation of major diameter (μm)	4.3	4.9	3.9
Average minor diameter (μm)	10.3	9.5	8.1
Standard deviation of minor diameter (μm)	2.5	2.9	2.3
Circularity	0.85	0.86	0.91
Feret diameter (μm)	14.1	12.8	10.4
Chl *a* (g/kg dry cell)	183.99 ± 16.35	19.21 ± 0.72	18.42 ± 0.43
Chl *b* (g/kg dry cell)	135.05 ± 10.81	28.93 ± 2.37	50.08 ± 0.24
Total Chl (g/kg dry cell)	319.04 ± 24.01	48.14 ± 2.95	68.50 ± 0.26
H–G asymmetry factor *g*	0.986	0.979	0.970

setups and analysis for measuring β_λ and κ_λ were validated for polystyrene microspheres with diameter of 5 μm and standard deviation of 0.6 μm supplied by Duke Scientific Corp., USA (Part No: 2005A). Experimental results were in good agreement with predictions from Mie theory assuming polystyrene to be non-absorbing. Details of the experimental setup, analysis, and validation can be found in Refs. [57,58].

4. Results and discussion

All normal–normal and normal–hemispherical transmittance measurements were performed twice and the arithmetic average of the results is reported. The relative difference between the replica measurements was less than 0.9% over the entire spectral region considered and for all microorganisms.

4.1. Cross-sections of *B. braunii*

Figs. 4(a), (c), and (e) show the absorption κ_λ, extinction β_λ, and scattering σ_λ coefficients of *B. braunii* measured at three different microorganism concentrations, namely 6.6986×10^{10}, 1.2796×10^{11}, and 2.2544×10^{11} cells/m^3 in the spectral region from 400 to 800 nm. Fig. 4(a) shows that *B. braunii* have absorption peaks at 435, 475, and 676 nm. The peaks at 435 and 676 nm correspond to the absorption peaks of in vivo chlorophyll *a* [69]. In addition in vivo chlorophyll *b* has absorption peaks at 475 and 650 nm [69]. Thus, the absorption peak at 475 nm and the peak broadening around 650 nm observed in Fig. 4(a) can be attributed to the presence of chlorophyll *b*. The chlorophyll *a* and *b* pigments are responsible for absorbing solar radiation and generating electrons that drive the metabolic reactions of the microorganisms.

In addition, Figs. 4(b), (d), and (f) show the spectral absorption, extinction, and scattering cross-sections $A_{abs,\lambda}$, $E_{ext,\lambda}$, and $S_{sca,\lambda}$ over the spectral region from 400 to 800 nm. The cross-sections $A_{abs,\lambda}$, $E_{ext,\lambda}$, and $S_{sca,\lambda}$ collapse on a single line for the two largest microorganism concentrations considered. This demonstrates that multiple scattering is negligible for the concentrations considered as assumed in the data analysis. Some wiggles in $S_{sca,\lambda}$ and $E_{ext,\lambda}$ can be observed for the smallest concentration resulting in relative difference less than 10% with the other two concentrations. This could be attributed to interferences within the cuvette occurring at low concentrations. Interferences do not occur for larger concentrations as the reflected beam is absorbed by the microorganisms and its intensity is much smaller than the incident beam. Overall, Figs. 4(b), (d), and (f) establishes that (1) the cross-sections $A_{abs,\lambda}$, $E_{ext,\lambda}$, and $S_{sca,\lambda}$ are independent of concentration X, (2) scattering dominates over absorption at all wavelengths between 400 and 800 nm.

4.2. Cross-sections of *Chlorella sp.*

Figs. 5(a), (c), and (e) show the absorption κ_λ, extinction β_λ, and scattering σ_λ coefficients of *Chlorella sp.* measured at three different concentrations, namely 2.9153×10^{11}, 3.1711×10^{11}, and 3.8985×10^{11} cells/m^3 in the spectral region from 400 to 800 nm. Here also, absorption peaks are apparent at 435, 475, and 676 nm corresponding to *Chl a* and *Chl b* as previously discussed for *B. braunii*. The difference lies in amplitude of the cross-sections which are smaller for *Chlorella sp.* for all wavelengths considered. This can be attributed to the fact that *Chlorella sp.* has smaller *Chl a* and *Chl b* concentrations than those of *B. braunii* as evident from Table 1. Indeed, *Chlorella sp.* has 90% and 78% less *Chl a* and *Chl b* concentrations than *B. braunii*, respectively.

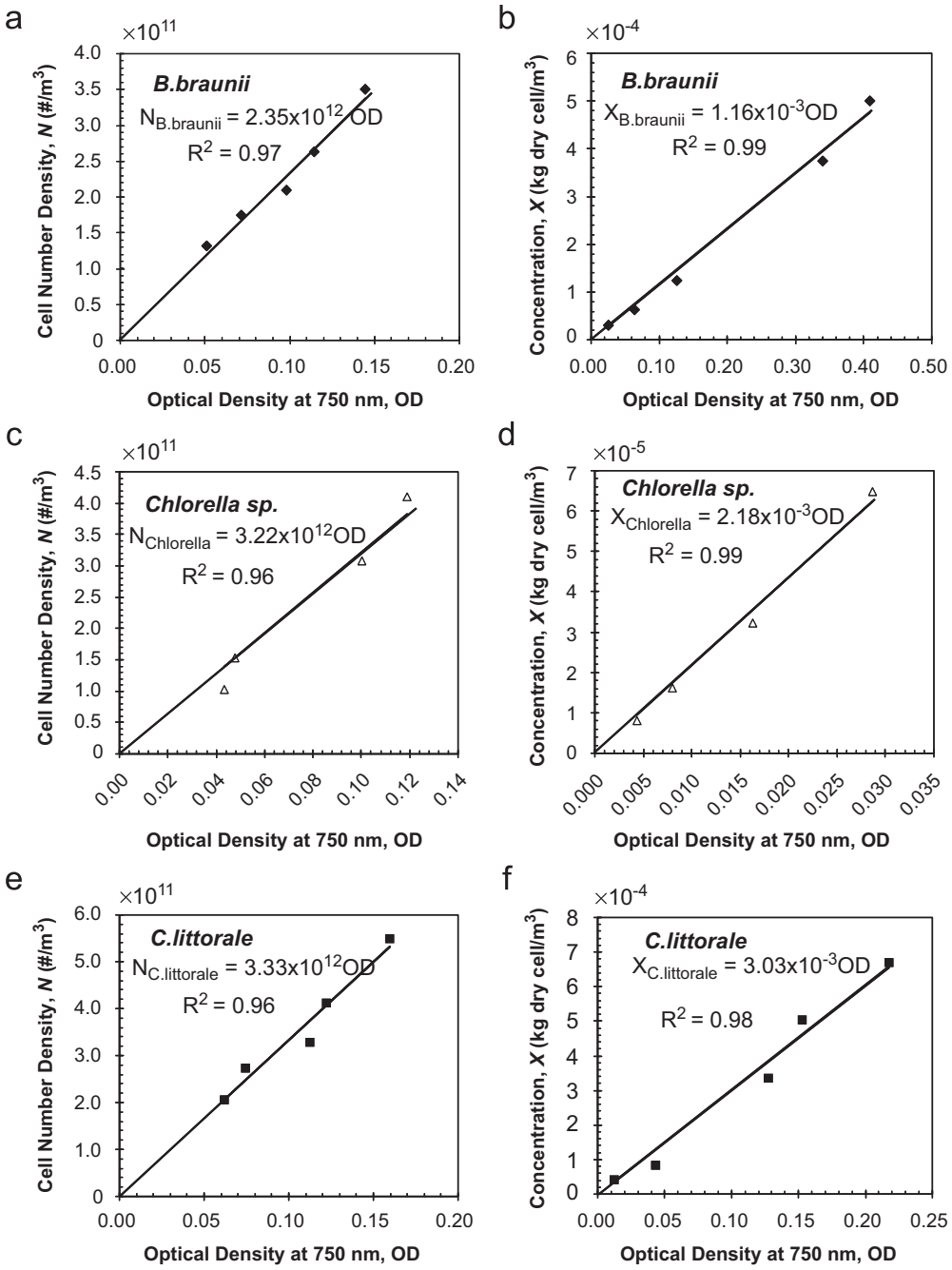

Fig. 3. Calibration curves showing cell density and dry weight concentration as functions of optical density (OD) at 750 nm and for 10 mm path length for (a, b) *B. braunii*, (c, d) *Chlorella sp.*, and (e, f) *C. littorale*.

4.3. Cross-sections of C. littorale

Figs. 6(a), (c), and (e) show the absorption κ_λ, extinction β_λ, and scattering σ_λ coefficients of *C. littorale* measured at three different concentrations, namely 3.2624×10^{11}, 3.6708×10^{11}, and 4.8106×10^{11} cells/m^3 in the spectral region from 400 to 800 nm. The same absorption peaks at 435, 475, and 676 nm corresponding to chlorophyll *a* and chlorophyll *b* are observed along with trends similar to those observed for *B. braunii* and *Chlorella sp.* for the extinction and scattering cross-sections.

The absorption cross-section of *C. littorale* is the smallest of the three microorganisms considered. Its scattering cross-section is larger than that of *Chlorella sp.* by 15% but smaller than that of *B. braunii* by 40–50%. This can be attributed to the complex and non-intuitive relationships between $A_{abs,\lambda}$, $E_{ext,\lambda}$, and $S_{sca,\lambda}$ and the chlorophyll concentrations and microorganisms size and shape.

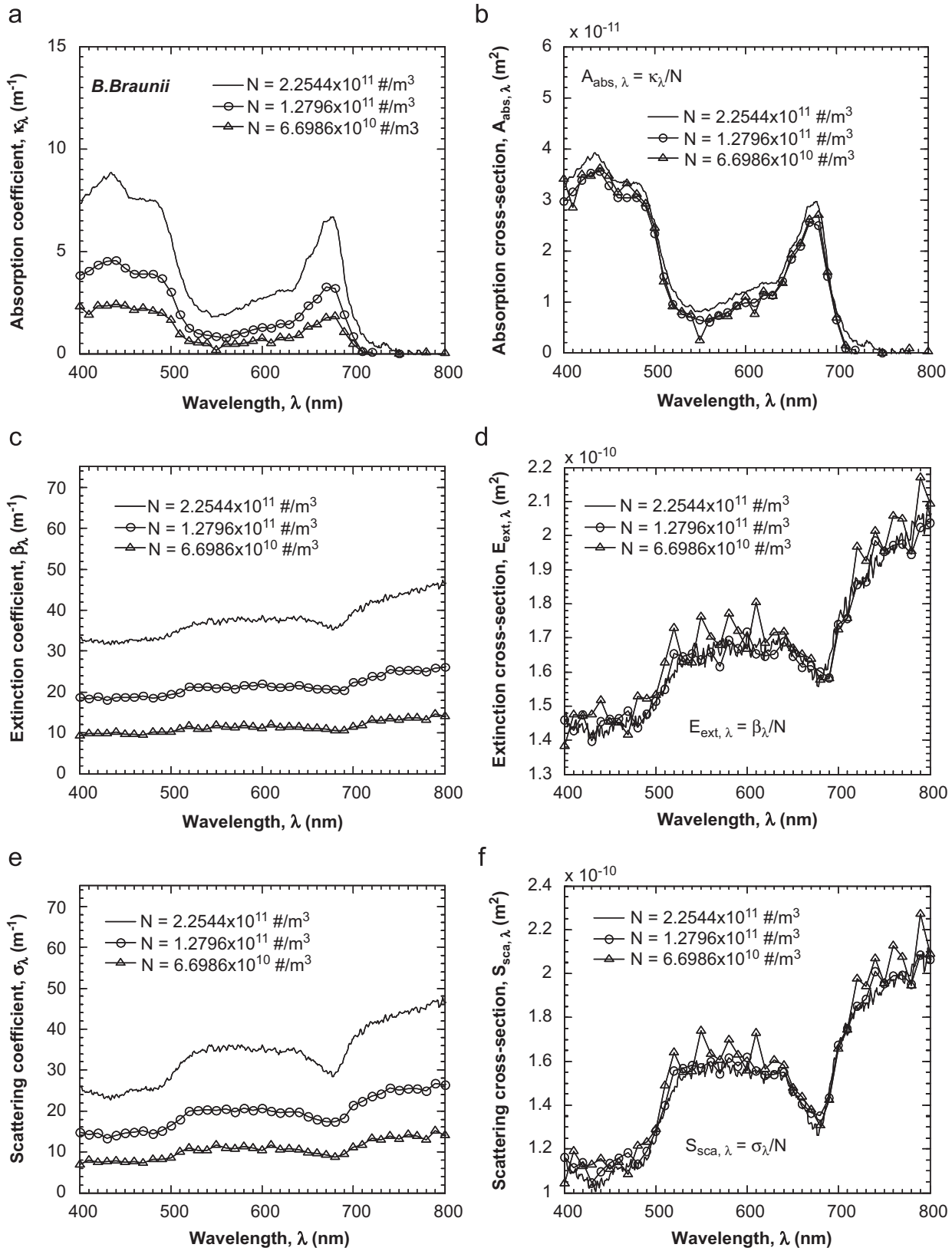

Fig. 4. The (a) absorption κ_λ, (c) extinction β_λ, and (d) scattering σ_λ coefficients and the corresponding (b) absorption $A_{abs,\lambda}$, (d) extinction $E_{ext,\lambda}$, and (f) scattering $S_{sca,\lambda}$ cross-sections of *B. braunii* over the spectral range from 400 to 800 nm at three different microorganism concentrations.

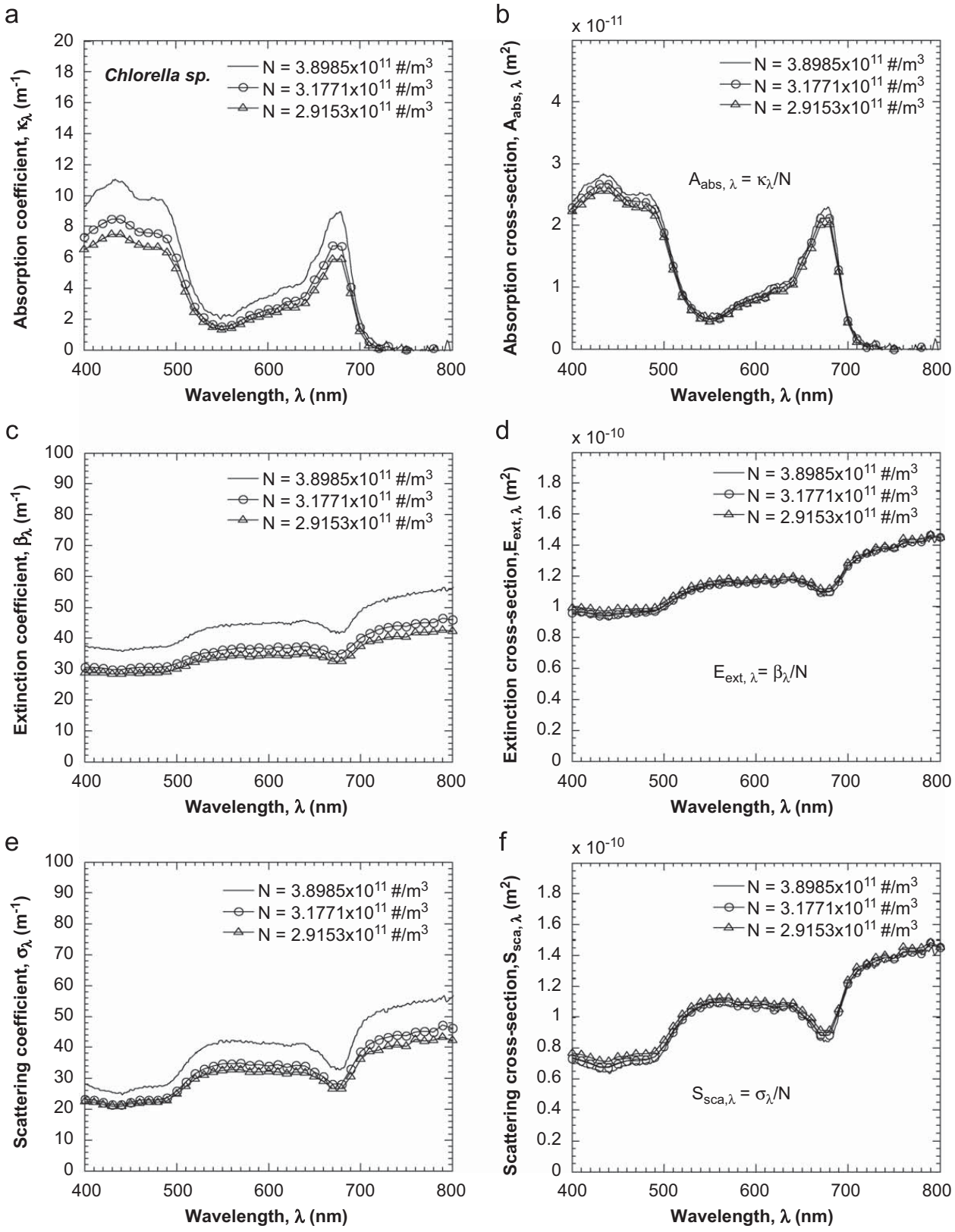

Fig. 5. The (a) absorption κ_λ, (c) extinction β_λ, and (d) scattering σ_λ coefficients and the corresponding (b) absorption $A_{abs,\lambda}$, (d) extinction $E_{ext,\lambda}$, and (f) scattering $S_{sca,\lambda}$ cross-sections of *Chlorella sp.* over the spectral range from 400 to 800 nm at three different microorganism concentrations.

Finally, Fig. 7 compares the spectral extinction coefficients $E_{ext,\lambda}$ and single scattering albedos ω_λ of *B. braunii*, *Chlorella sp.*, and *C. littorale* as a function of wavelength between 400 and 800 nm. A slight increase in $E_{ext,\lambda}$ with wavelength can be observed for all algae with a dip between 670 and 680 nm. The extinction coefficient of *Chlorella sp.* falls within 10% of that of *C. littorale* while that of *B. braunii* is larger than the others by at least 40% and up to 70% over the spectral range of

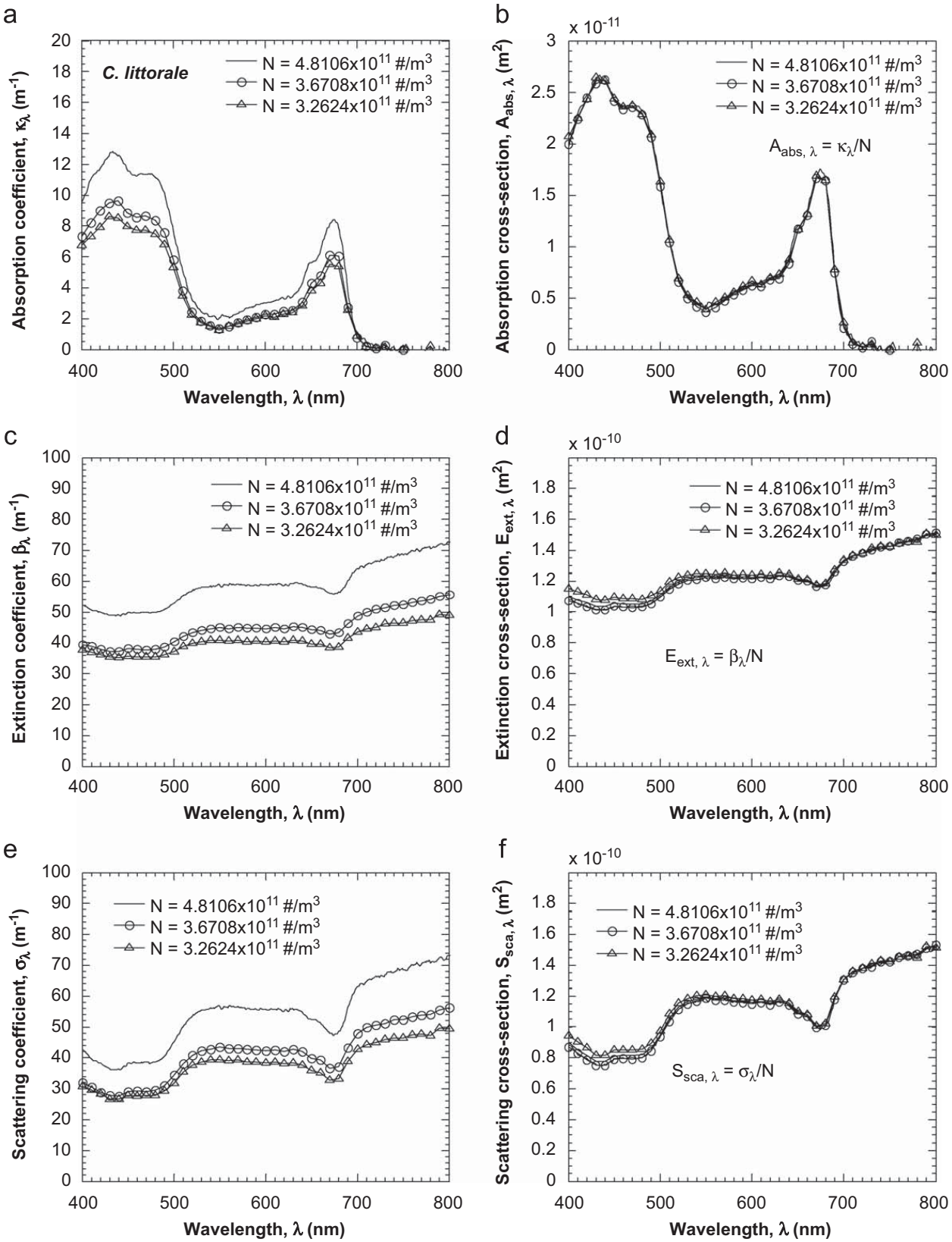

Fig. 6. The (a) absorption κ_λ, (c) extinction β_λ, and (d) scattering σ_λ coefficients and the corresponding (b) absorption $A_{abs,\lambda}$, (d) extinction $E_{ext,\lambda}$, and (f) scattering $S_{sca,\lambda}$ cross-sections of *C. littorale* over the spectral range from 400 to 800 nm at three different microorganism concentrations.

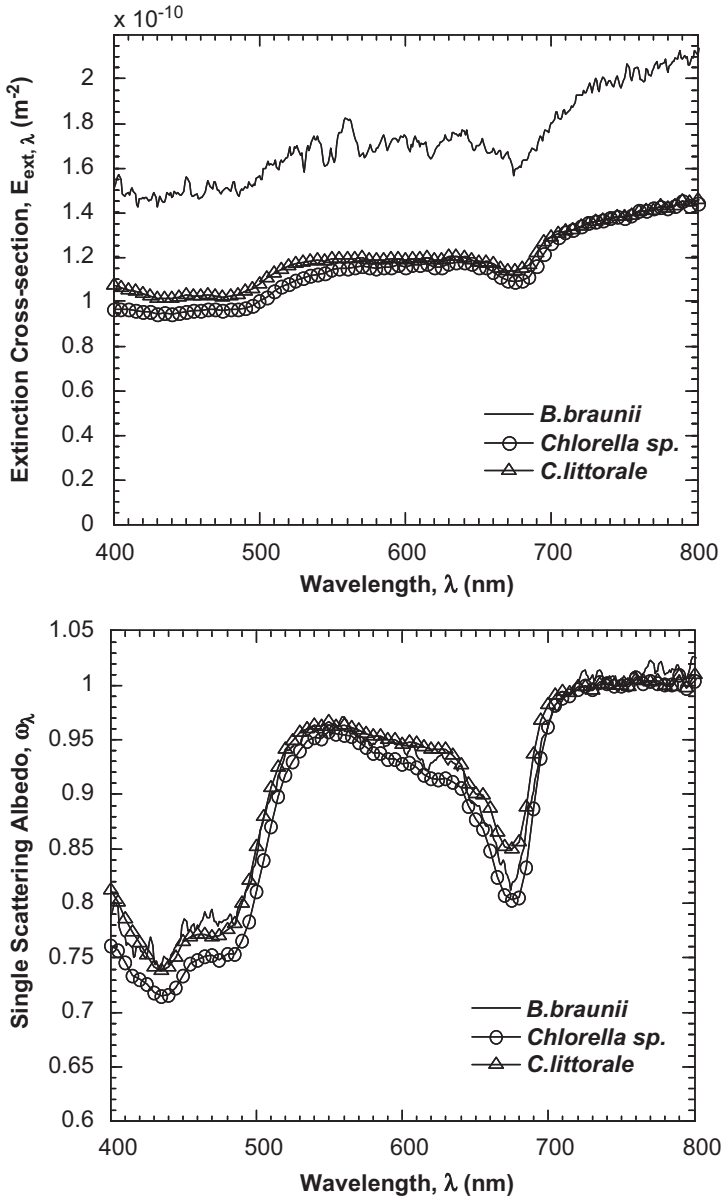

Fig. 7. Average extinction coefficient and single scattering albedo of *B. braunii*, *Chlorella sp*., and *C. littorale* between 400 and 800 nm.

interest. On the contrary, the single scattering albedos of the three microorganisms fall within less than 8% of each other. In all cases, ω is larger than 0.7 indicating that scattering dominates over absorption.

4.4. Scattering phase functions of all strains

Finally, the scattering phase functions of the three microorganisms of interest were measured using the nephelometer described in detail in Refs. [57]. Due to the finite size of the probe and the beam, data could only be obtained for scattering angle Θ up to 140° where the probe does not block the incident beam. Fig. 8 shows the scattering phase functions of *B. braunii*, *Chlorella sp*., and *C. littorale* measured by the nephelometer along with the Henyey–Greenstein scattering phase function (HG). The latter is given by [49]

$$\Phi_{HG} = \frac{1-g^2}{[1+g^2-2g\cos\Theta]^{3/2}} \tag{7}$$

where g is the Henyey–Greenstein asymmetry factor defined as the mean cosine of the experimentally measured scattering phase function [19] and was computed for each strain. Its values for each strain are summarized in Table 1.

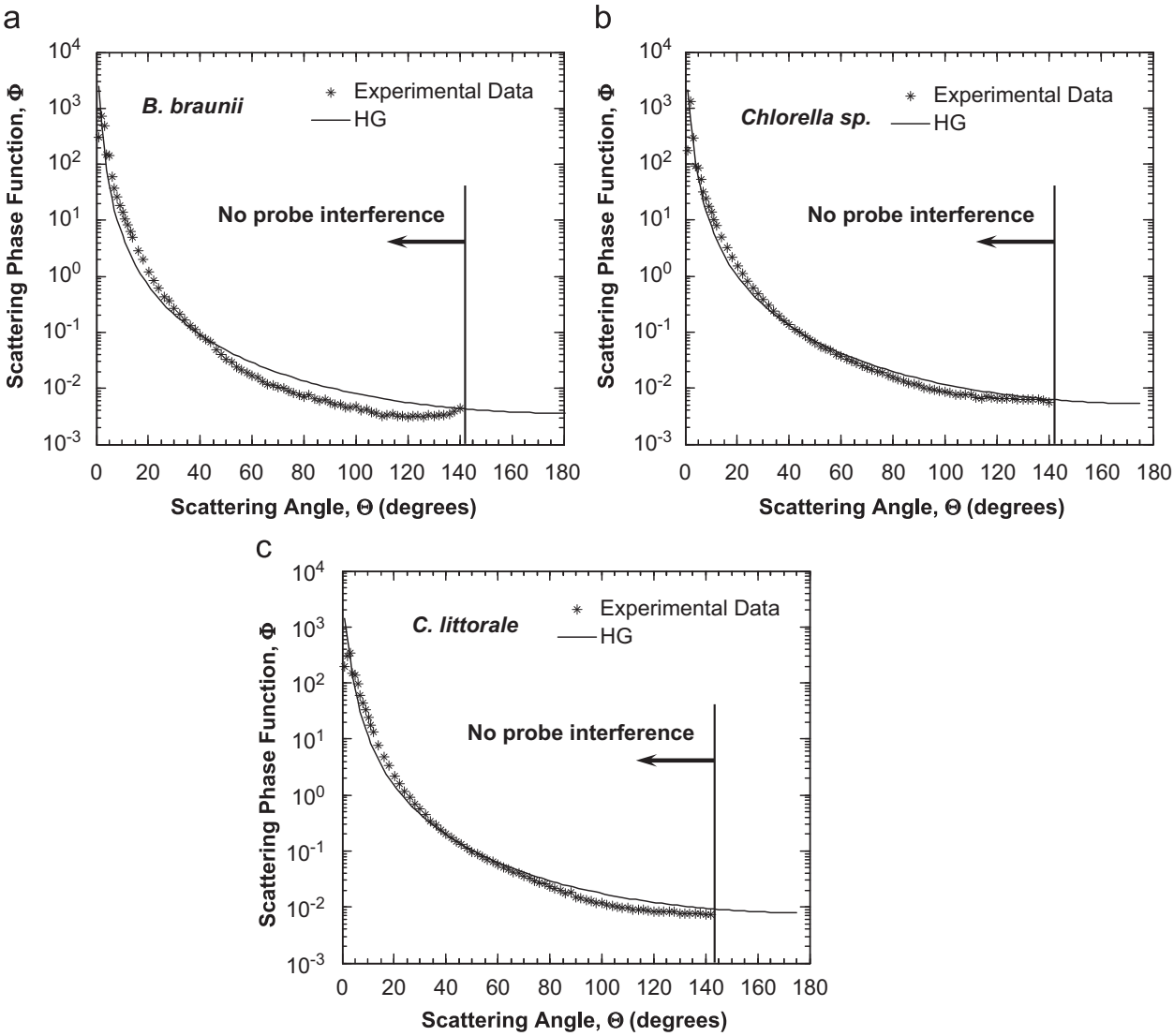

Fig. 8. The scattering phase function of (a) *B. braunii*, (b) *Chlorella sp.*, and (c) *C. littorale* at 632.8 nm obtained experimentally and the corresponding HG approximation.

5. Conclusion

This paper has been concerned with experimental measurements of the radiation characteristics of three species of CO_2 consuming algae with large oil and protein content namely *B. braunii*, *Chlorella sp.*, and *C. littorale*. Such data are difficult to predict theoretically and are essential to the design and scaling of industrial systems for CO_2 fixation and biofuel production as well as for controlled ecological life support systems. Experimental results establish that for all strains, scattering dominates over absorption. The magnitudes of the extinction and scattering cross-section are functions of the size, shape, and chlorophyll content of each strains in a non-trivial manner. Absorption peaks at 435, 475, and 676 nm corresponding to chlorophyll *a* and chlorophyll *b* have been clearly identified.

References

[1] IPPC. Climate change 2007: impacts, adaptation and vulnerability. Contribution of working group II to the fourth assessment report of the intergovernmental panel on climate change. Cambridge, UK: Cambridge University Press; 2007.
[2] US Central Intelligence Agency. The world factbook 2008 ⟨https://www.cia.gov/cia/publications/factbook/index.html⟩, 2008.
[3] Energy Information Administration. Short term energy outlook ⟨http://www.eia.doe.gov/oiaf/forecasting.html⟩, 2008.
[4] Yamasaki A. An overview of CO_2 mitigation options for global warming—emphasizing CO_2 sequestration options. Journal of Chemical Engineering of Japan 2003;34(4):361–75.
[5] Peters W, Jacobson AR, Sweeney C, Andrews AE, Conway TJ, Masarie L, et al. An atmospheric perspective on North American carbon dioxide exchange: carbon tracker. Proceedings of the National Academy of Science 2007;27(48):18925–30.
[6] Cook PJ. Greenhouse gas technologies: a pathway to decreasing carbon intensity. In: Collings AF, Critchley C, editors. Artificial photosynthesis: from basic biology to industrial applications. Weinheim, Germany: Wiley-VCH Verlag GmbH; 2005. p. 301–8.
[7] Ohsumi T. CO_2 disposal options in deep sea. Marine Technology Society Journal 1995;29(3):58–66.

[8] Ishibashi M, Ota H, Akutsu N, Umeda S, Tajika M, Izumi J. Technology for removing carbon dioxide from power plant flue gas by the physical adsorption model. Energy Conversion and Management 1996;37(6–8):929–33.
[9] Judkins R, Burchell T. CO_2 removal from gas streams using a carbon fiber composite molecular sieve. In: First national conference on carbon sequestration. Washington, DC: National Energy Technology Laboratory; May 14–17, 2001.
[10] Herzog H. What is the future for carbon capture and sequestration? Environmental Science and Technology 2001;35(7):148A–53A.
[11] Bill A, Wokaun A, Eliasson B, Killer E, Koegelschatz U. Greenhouse gas chemistry. Energy Conversion Management 1997;38:S415–22.
[12] Kaneco S, Iiba K, Yabuuchi M, Nishio N, Ohnishi H, Katsumata H, et al. High efficiency electrochemical CO_2-to-methane conversion method using methanol with lithium supporting electrolytes. Industrial and Engineering Chemistry Research 2002;41(21):5165–70.
[13] Abe Y, Kojima T, Yamada K. A large scale afforestation in arid land as countermeasures for CO_2. Journal of Arid Land Studies 1997;7:77–81.
[14] Chelf P, Brown LM, Wyman CE. Aquatic biomass resources and carbon dioxide trapping. Biomass and Bioenergy 1993;4(3):175–83.
[15] Martin JH, Fitzwater SE. Iron defficiency limits phytoplankton growth in the North-East Pacific subarctic. Nature 1988;331(6154):341–3.
[16] Nozaki Y. The role of carbon cycling. Tokyo, Japan: University of Tokyo Press; 1993.
[17] Chishlom SW, Falkowski PG, Cullen JJ. Discrediting ocean fertilization. Science 2001;294:309–10.
[18] Seifritz W. CO_2 disposal by means of silicates. Nature 1990;345(6275):486.
[19] Kojima T, Nagamine A, Ueno N, Uemiya S. Absorption and fixation of carbon dioxide by rock weathering. Energy Conversion and Management 1997;38:S461–6.
[20] Pace RJ. An integrated artificial photosynthesis model. In: Collings AF, Critchley C, editors. Artificial photosynthesis: from basic biology to industrial applications. Weinheim, Germany: Wiley-VCH Verlag GmbH; 2005. p. 13–34.
[21] Bolton JR, Hall DO. The maximum efficiency of photosynthesis. Photochemistry and Photobiology 1991;53(4):545–8.
[22] Kurano N, Ikemoto H, Miyashita H, Hasegawa I, Hata H, Miyachi S. Fixation and utilization of carbon dioxide by microalgal photosynthesis. Energy Conversion Management 1995;36(6–9):689–92.
[23] Vanek F, Albright LD. Energy systems engineering: evaluation and implementation. New York, NY: McGraw-Hill Professional; 2008.
[24] Stewart C, Hessami MA. A study of methods of carbon dioxide capture and sequestration—the sustainability of a photosynthetic bioreactor approach. Energy Conversion and Management 2005;46(3):403–20.
[25] Hirata S, Hayashitani M, Taya M, Tone S. Carbon dioxide fixation in batch culture of *Chlorella sp*. using a photobioreactor with a sunlight-collection device. Journal of Fermentation and Bioengineering 1996;81(5):470–2.
[26] Keffer JE, Kleinheinz GT. Use of *Chlorella vulgaris* for CO_2 mitigation in a photobioreactor. Journal of Industrial Microbiology and Biotechnology 2002;29(5):275–80.
[27] Yoon JH, Sim SJ, Kim MS, Park TH. High cell density culture of *Anabaena variabilis* using repeated injections of carbon dioxide for the production of hydrogen. International Journal of Hydrogen Energy 2002;27(11–12):1265–70.
[28] Skjånes K, Lindblad P, Muller J. BioCO_2—a multidisciplinary, biological approach using solar energy to capture CO_2 while producing H_2 and high value products. Biomolecular Engineering 2007;24(4):405–13.
[29] Hall DO, Markov SA, Watanabe Y, Rao KK. The potential applications of cyanobacterial photosynthesis for clean technologies. Photosynthesis Research 1995;46(1–2):159–67.
[30] Melis A, Neidhardt J, Benemann JR. *Dunaliella salina* (*Chlorophyta*) with small chlorophyll antenna sizes exhibit higher photosynthetic productivities and photon use efficiencies than normally pigmented cells. Journal of Applied Phycology 1999;10(6):515–25.
[31] Nakajima Y, Ueda R. The effect of reducing light-harvesting pigment on marine microalgal productivity. Journal of Applied Phycology 2000;12(3–5):285–90.
[32] Ogbonna JC, Soejima T, Tanaka H. An integrated solar and artificial light system for internal illumination of photobioreactors. Journal of Biotechnology 1999;70(1–3):289–97.
[33] Lee J-S, Lee J-P. Review of advances in biological CO_2 mitigation technology. Biotechnology and Bioprocess Engineering 2003;8(6):354–9.
[34] Ai W, Guo S, Qin L, Tang Y. Development of ground-based space micro-algae photobioreactor. Advances in Space Research 2008;41(5):742–7.
[35] Javanmardian M, Palsson BØ. Design and operation of an algal photobioreactor system. Advances in Space Research 1992;12(5):231–5.
[36] Sheehan J, Dunahay T, Benemann J, Roessler P. A look back at the U.S. Department of Energy's aquatic species program—biodiesel from algae. Close-Out Report, NREL/TP-580-24190; 1998.
[37] Murakami M, Ikenouchi M. The biological CO_2 fixation and utilization project by rite (2)—screening and breeding of microalgae with high capability in fixing CO_2. Energy Conversion and Management 1997;38(Suppl.):S493–7.
[38] Metzger P, Largeau C. *Botryococcus braunii*: a rich source for hydrocarbons and related ether lipids. Applied Microbiology and Biotechnology 2005;66(5):486–96.
[39] Metzger P, Berkaloof C, Casadevall E, Coute A. Alkadiene- and botryococcene producing races of wild strains of *Botryococcus braunii*. Phytochemistry 1985;24(10):2305–20.
[40] Sawayama S, Inoue S, Yokoyama S. Continuous culture of hydrocarbon-rich microalga *Botryococcus braunii* in secondarily treated sewage. Applied Microbiology and Biotechnology 1994;41(6):729–31.
[41] Chisti Y. Biodiesel from microalgae. Biotechnology Advances 2007;25(3):294–306.
[42] Hillen LW, Pollard G, Wake LV, White N. Hydrocracking of the oils of *Botryococcus braunii* to transport fuels. Biotechnology and Bioengineering 1982;24(1):193–205.
[43] Lee JY, Kwon TS, Baek K, Yang JW. Biological fixation of CO_2 by *Chlorella sp*. HA-1 in a semi-continuous and series reactor system. Journal of Microbiology and Biotechnology 2005;15(3):461–5.
[44] Chiu SY, Kao CY, Chen CH, Kuan TC, Ong SC, Lin CS. Reduction of CO_2 by a high-density culture of *Chlorella sp*. in a semicontinuous photobioreactor. Bioresource Technology 2008;99(9):3389–96.
[45] Kodama M, Ikemoto H, Miyachi S. A new species of highly CO_2-tolerant fast growing marine microalga suitable for high density culture. Journal of Marine Biotechnology 1993;1:21–5.
[46] Hu Q, Kurano K, Kawachi M, Iwasaki I, Miyachi S. Ultrahigh cell density culture of a marine green algae *Chlorococcum littorale* in a flat plate photobioreactor. Applied Microbiology and Biotechnology 1998;49(6):655–62.
[47] Vunjak-Novakovic G, Kim Y, Wu XX, Berzin I, Merchuk JC. Air-lift bioreactors for algal growth on flue gas: mathematical modeling and pilot-plant studies. Industrial and Engineering Chemistry Research 2005;44(16):6154–63.
[48] Pulz O. Evaluation of GreenFuel's 3D matrix algae growth engineering scale unit—APS Red Hawk Unit AZ. Greenfuels Performance Summary Report ⟨www.greenfuelonline.com/gf_files/Performance%20Summary%20Report.pdf⟩; September 2007.
[49] Modest MF. Radiative heat transfer. San Diego, CA: Academic Press; 2003.
[50] Stramski D, Mobley CD. Effect of microbial particles on oceanic optics: a database of single-particle optical properties. Limnology and Oceanography 1997;42(3):538–49.
[51] Davies-Colley RJ, Pridmore RD, Hewitt JE. Optical properties and reflectance spectra of 3 shallow lakes obtained from a spectrophotometric study. New Zealand Journal of Marine and Freshwater Research 1983;17:445–59.
[52] Bricaud A, Morel A, Prieur L. Optical efficiency factors of some phytoplankters. Limnology and Oceanography 1983;28(5):816–32.
[53] Agrawal BM, Mengüç MP. Forward and inverse analysis of single and multiple scattering of collimated radiation in an axisymmetric system. International Journal of Heat and Mass Transfer 1991;34(3):633–47.
[54] Jonasz M, Fournier GR. Light scattering by particles in water: theoretical and experimental foundations. San Diego, CA: Academic Press; 2007.
[55] Privoznik KG, Daniel KJ, Incropera FP. Absorption, extinction, and phase function measurements for algal suspensions of *Chlorella pyrenoidosa*. Journal of Quantitative Spectroscopy and Radiation Transfer 1978;20(4):345–52.

[56] Daniel KJ, Laurendeau NM, Incropera FP. Prediction of radiation absorption and scattering in turbid water bodies. Transaction of the ASME—Journal of Heat Transfer 1979;101(1):63–7.
[57] Berberoğlu H, Pilon L. Experimental measurement of the radiation characteristics of *Anabaena variabilis* ATCC 29413-U and *Rhodobacter sphaeroides* ATCC 49419. International Journal of Hydrogen Energy 2007;32(18):4772–85.
[58] Berberoğlu H, Pilon L, Melis A. Radiation characteristics of *Chlamydomonas reinhardtii* CC125 and its truncated chlorophyll antenna transformants tla1, tlaX, and tla1-CW^{+}. International Journal of Hydrogen Energy 2008;33(22):6467–83.
[59] Berberoğlu H, Yin J, Pilon L. Simulating light transfer in a bubble sparged photobioreactor for simultaneous hydrogen fuel production and CO_2 mitigation. International Journal of Hydrogen Energy 2007;32(13):2273–85.
[60] Moore C, Seneveld RV, Kitchen JC. Preliminary results from an in situ spectral absorption meter. Proceedings of SPIE 1992;1750:330–7.
[61] Zaneveld JRV, Bartz R, Kitchen JC. Reflective tube absorption meter. Proceedings of SPIE 1990;1302:124–36.
[62] Maffione RA, Voss KJ, Honey RC. Measurement of the spectral absorption coefficient in the ocean with an isotropic source. Applied Optics 1993;32(18):3273–9.
[63] UTEX the culture Collection of Algae, section media ⟨http://www.utex.org⟩, 2008.
[64] Rasband WS. Image J. U.S. National Institute of Health, Bethesda, MD, USA ⟨http://rsb.info.nih.gov/ij/⟩, 1997–2007.
[65] Quirantes A, Bernard S. Light scattering by marine algae: two-layer spherical and nonspherical models. Journal of Quantitative Spectroscopy and Radiative Transfer 2004;89(1–4):311–21.
[66] Harris EH. The chlamydomonas sourcebook. New York, NY: Academic Press; 1989.
[67] Bohren CF, Huffman DR. Absorption and scattering of light by small particles. New York, NY: Wiley; 1998.
[68] Lee SC. Scattering phase function for fibrous media. International Journal of Heat and Mass Transfer 1990;33(10):2183–90.
[69] Ke B. Photosynthesis, photobiochemistry and photobiophysics. Dordrecht, The Netherlands: Kluwer Academic Publishers; 2001.